Smeared crack approach for asphalt concrete

Rongzong Wu[a,*], John Harvey[b]

[a]Pavement Research Center, ITS, Richmond, CA 94804–4603, USA
[b]Pavement Research Center, University of California, Davis, CA 95616, USA

Abstract

This paper discusses the applicability of cohesive crack model to asphalt concrete as a composite material. A smeared crack approach to the cohesive crack model for linear viscoelastic material with rate-dependent cracking is presented in detail. Numerical examples with FEM simulation for uniaxial tension and beam bending tests were then given to demonstrate the capability of the approach.

Keywords: Smeared crack approach; Asphalt concrete; Finite element; Spurious mesh dependency; Viscoelastic; Cohesive zone model

1. Introduction

Mechanistic modeling of cracking in asphalt concrete has been an open topic for a long time. Although the classical fracture mechanics, e.g. LEFM, became well established around 1980 [1], their application to asphalt concrete has been only limited, if not completely unsuccessful. This probably implies that classical fracture mechanics are not well suited for asphalt concrete.

In classical fracture mechanics, materials are homogeneous and the crack tip non-linear field has to be small relative to the structure dimension. However, asphalt concrete is a composite, with the nominal size of large aggregates in the order of 1/3 to 1/20 of the structure size (namely, the layer thickness in a pavement).

The essence of fracture mechanics is the principle that cracking is driven by energy rather than by strain or stress. When the crack-tip field is small enough, the energy balance can be expressed by using a single parameter (e.g. stress intensity factor K). In other cases, one would have to model the crack-tip field directly. One of the choices is to adopt the cohesive crack model (or fictitious crack model, cohesive zone model), see e.g. [2,3,4].

The cohesive crack model assumes that there is a bridging stress across the crack faces, and the stress-separation curve is a material property. One can derive the energy required to advance a unit area of crack surface based on the stress-separation curve.

The classical cohesive crack model has no rate-dependency and needs to be extended. There are two different rate-dependencies: one from the bulk material between cracks, the other from the cracking itself. The model proposed herein covers both of the two rate-dependencies to facilitate modeling cracking in asphalt concrete.

When the cohesive crack model is implemented in the finite element method (FEM), cracks can be represented in a discrete manner (by splitting the nodes along crack path) or in a continuum manner (by superposing the crack separation onto the strain of the cracked element). The former is usually referred to as *discrete crack approach* as oppose to *smeared crack approach* for the latter. These two approaches practically yield the same result and smeared crack approach is adopted here.

This paper first describes the formulation of a smeared crack approach for linear viscoelastic material with rate-dependent cracking. It then gives examples of its application to asphalt concrete.

2. Constitutive relationship for smeared crack approach

2.1. The framework

The basic idea for a smeared crack approach is the strain decomposition [5]:

$$\varepsilon = \varepsilon^b + \varepsilon^f \tag{1}$$

* Corresponding author. Tel.: +1 510 231 5753; Fax: +1 510 231 9589; E-mail: wurong@berkeley.edu

Computational Fluid and Solid Mechanics 2005
K.J. Bathe (Editor)

where ε^b is the bulk strain for the solid material between cracks and ε^f is the strain for the cracks. The relation between ε^b and the total stress σ is determined by the intact solid material property, while ε^f determines the traction acting on the cracking surface following a stress-separation curve. Suppose the normal to the cracking surface is $\boldsymbol{n}$, then the traction on the crack surface $\tau = \sigma \cdot \boldsymbol{n}$ is uniquely determined by the cracking strain ε^f.

For a linear viscoelastic bulk material represented by generalized Maxwell element (GME), if it is assumed that the strain varies linearly between current time t and the last time step t_n in a FEM solution setting, then the stress–strain relation for the bulk material can be expressed as:

$$\sigma = \boldsymbol{D}(\Delta t) : \varepsilon^b + \sigma_n(\Delta t, \varepsilon^b_n) \tag{2}$$

The stiffness tensor $\boldsymbol{D}(\Delta t)$ has exactly the same structure as in linear elasticity:

$$D_{ijkl} = \lambda(\Delta t)\delta_{ij}\delta_{kl} + \mu(\Delta t)(\delta_{ik}\delta_{jl} + \delta_{il}\delta_{jk}) \tag{3}$$

The expression for the bulk strain now becomes:

$$\varepsilon^b = \boldsymbol{D}^{-1}(\Delta t) : \sigma - \boldsymbol{D}^{-1}(\Delta t) : \sigma_n(\Delta t, \varepsilon^b_n) \tag{4}$$

For illustration purposes, assume that the normal of the cracking plane coincides with the x-axis of the coordinate system. Then the traction on the cracking plane can be decomposed along the three coordinate axes:

$$\tau = \sigma_{xx}e_x + \sigma_{xy}e_y + \sigma_{xz}e_z \tag{5}$$

and the cracking strain tensor has only three independent non-zero components: ε^f_{xx}, ε^f_{xf} and ε^f_{xx}. Three more equations are required to solve these three additional unknowns. Following the procedure in [6], define two cracking compliances C_N and C_T such that:

$$\varepsilon^f_{xx} = C_N\sigma_{xx} \tag{6}$$

and

$$\varepsilon^f_{xy} = C_T\sigma_{xy} \text{ and } \varepsilon^f_{xz} = C_T\sigma_{xz} \tag{7}$$

Denoting the second term in the right hand side of Eq. (4) as the residual strain ϵ^r, and combining Eqs. (1), (4), (6), and (7), one can reach the following constitutive relationship:

$$\begin{Bmatrix} \varepsilon_{xx} \\ \varepsilon_{yy} \\ \varepsilon_{zz} \end{Bmatrix} = \frac{1}{E(\Delta t)} \begin{bmatrix} 1 + E(\Delta t)C_N & -\nu & -\nu \\ -\nu & 1 & -\nu \\ -\nu & -\nu & 1 \end{bmatrix} \begin{Bmatrix} \sigma_{xx} \\ \sigma_{yy} \\ \sigma_{zz} \end{Bmatrix} - \begin{Bmatrix} \varepsilon^r_{xx} \\ \varepsilon^r_{yy} \\ \varepsilon^r_{zz} \end{Bmatrix} \tag{8}$$

and:

$$\begin{Bmatrix} \gamma_{xy} \\ \gamma_{yz} \\ \varepsilon_{zx} \end{Bmatrix} = \frac{1}{G(\Delta t)} \begin{bmatrix} 1 + G(\Delta t)C_T 0 & 0 & 0 \\ 0 & 1 & 0 \\ 0 & 01 & +G(\Delta t)C_T \end{bmatrix} \begin{Bmatrix} \sigma_{xy} \\ \sigma_{yz} \\ \sigma_{zx} \end{Bmatrix} - \begin{Bmatrix} \gamma^r_{xy} \\ \gamma^r_{yz} \\ \gamma^r_{zx} \end{Bmatrix} \tag{9}$$

The question remains on how to determine the two cracking compliances. This is solved by using the stress-separation curve of the material.

2.2. Stress-separation curve

The question at hand is to determine the cracking stress from the cracking strain. This can be done by providing a potential function as shown in [7], where the following stress-separation curve was reached:

$$\sigma = f_t\beta\delta\exp(1 - \beta\delta) \tag{10}$$

where f_t is the peak cracking stress, δ is the crack separation, which depends on both normal opening and shear sliding, and β is a material property that determines the shape of the function. This stress-separation curve is adopted at the beginning of this study with the simplification that δ is equivalent to the *opening* displacement alone. And furthermore, since crack displacement is smeared across the cracking element thickness w_c along the normal to the cracking plane, Eq. (10) is recast into:

$$\sigma_{xx} = f_t\beta'\varepsilon^f_{xx}\exp(1 - \beta'\varepsilon^f_{xx}) \tag{11}$$

where $\beta' = \beta \cdot w_c$. Since w_c depends on the specific FEM discretization, the stress-separation function is specific to a certain FEM mesh. This simple trick removes the spurious mesh-dependency of continuum mechanics methods (smeared crack approach being one of them) when applied to localized failure problem.

To account for the rate dependency of cracking behavior, add an additional term to Eq. (11):

$$\sigma_{xx} = (f_t + \eta'\dot{\varepsilon}^f_{xx})\beta'\varepsilon^f_{xx}\exp(1 - \beta'\varepsilon^f_{xx}) \tag{12}$$

where η' is the mesh specific rate effect parameter and $\eta' = \eta \cdot w_c$ when η is the corresponding material property. This modification is in essence increasing the peak stress for the stress-separation curve.

Equation (12) was first adopted in this study. However, it was later found that the following simpler form actually fits the experimental data better and Eq. (13) is used instead in this paper:

$$\sigma_{xx} = (f_t + \eta'\dot{\varepsilon}^f_{xx})\exp(-\beta'\varepsilon^f_{xx}) \tag{13}$$

Apparently, C_N can be determined from Eq. (13), and C_T can simply be assumed to be $2(1 + \nu)C_N$ in parallel to linear elasticity.

A physical analogy of the constitutive model can be illustrated as in Fig. 1. Note that in Fig. 1, the dashpot in parallel with the cracking element is actually nonlinear. It will vanish after the material is completely cracked.

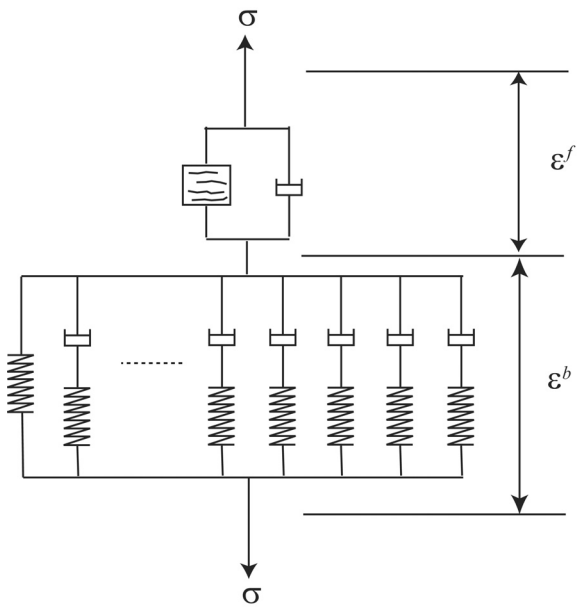

Fig. 1. Physical analogy of the constitutive model.

3. Examples

The proposed smeared crack approach was implemented in FEAP [8] by providing a user constitutive module. A dense graded asphalt concrete with AR-8000 binder was used in this simulation. The volumetric response of the bulk material was assumed to be linear elastic, while the deviatoric response was represented by generalized Maxwell model with the parameters listed in Table 1. The instant shear modulus is $G = 17{,}682$ MPa; the volumetric modulus is $K = 53{,}045$ MPa. The stress-separation curve parameters are: $f_t = 1.9$ MPa, $\beta = 2.14\,\text{mm}^{-1}$, $\eta = 100$ MPa/(s.mm). Both examples were simulated with plane stress model.

3.1. Uniaxial pension tests

A core 8″ high with 4″ diameter is subjected to uniaxial tension under different nominal axial strain rates. The nominal stress-strain curves for different nominal strain rates are shown in Fig. 2.

3.2. SHRP fatigue beam monotonic bending test

Monotonic third point bending tests under displacement control were simulated for SHRP fatigue beams [9]. The effective geometry of the beams were $354 \times 51 \times 65\,\text{mm}^3$. As in typical SHRP fatigue beam tests, the load was applied at the third division points and the vertical actuator pressed down the beam at a constant vertical displacement rate.

The measured and calculated load-displacement curves are shown in Fig. 3.

4. Summary

This paper presents a smeared crack approach of cohesive crack model for a linear viscoelastic material with rate-dependent cracking. The preliminary simulations showed great promise in capturing the cracking behavior of asphalt concrete.

Table 1
Model parameters for AR-8000 mix

Branch no. i	Relaxation time λ_i(sec)	Shear modulus ratio $\gamma i = G_i/G$
1	5.0E−6	3.7083E−001
2	5.0E−5	2.9125E−001
3	5.0E−4	3.3448E−002
4	5.0E−3	9.1920E−002
5	5.0E−2	9.1825E−002
6	5.0E−1	6.8851E−002
7	5.0E+0	3.6593E−002
8	5.0E+1	1.1081E−002
9	5.0E+2	3.2054E−003

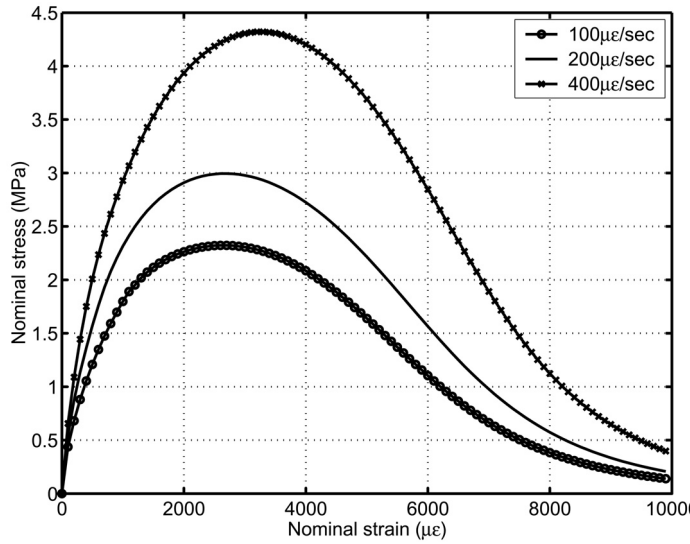

Fig. 2. Nominal stress-strain curves for uniaxial tension tests under different nominal strain rates.

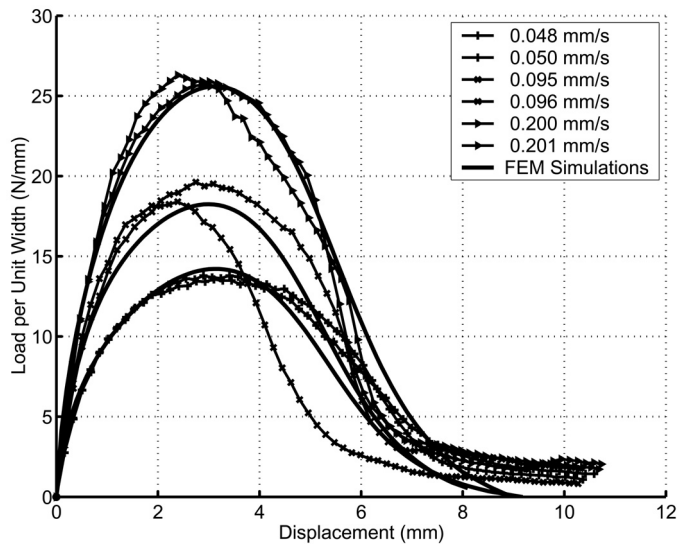

Fig. 3. Actual and simulated load-displacement curves for SHRP fatigue beam monotonic bending test under different displacement rates.

Acknowledgment

Financial support provided by the California Department of Transportation (CAL-TRANS) is gratefully appreciated.

References

[1] Anderson TL. Fracture Mechanics, 2nd edition. Boca Ralton, FL: CRC Press, 1995, p. 12.

[2] Hillerborg A, Modeer RM, Petersson PE. Analysis of crack formation and crack growth in concrete by means of fracture mechanics and finite elements. Cement and Concrete Research 1976;6:773–782.

[3] Jenq YS, Perng JD. Analysis of crack propagation in asphalt concrete using cohesive crack model. Transportation Research Record 1991;1317:90–99.

[4] Jenq YS, Liaw CJ, Pei L. Analysis of crack resistance of asphalt concrete overlays–a fracture mechanics approach. Transportation Research Record 1993;1388:160–166.

[5] Rots JG. Computational Modeling of Concrete Fracture, Delft University of Technology, PhD Dissertation, 1988.
[6] Bazant ZP, Planas J. Fracture and Size Effect in Concrete and Other Quasibrittle Materials, Boca Ralton, FL: CRC Press, 1998, p. 236.
[7] de-Andres A, Perez JL, Ortiz M. Elastoplastic finite element analysis of three-dimensional fatigue crack growth in aluminium shafts subjected to axial loading. Int J of Solids and Structure 1999;36:2231–2258.
[8] Taylor RL. FEAP–A Finite Element Analysis Program, http://www.ce.berkeley.edu/~rlt/feap/, 2003.
[9] Tayebali A, Deacon JA, Monosmith CL. Development and evaluation of dynamic flexural beam fatigue test system. Transportation Research Record 1996;1545:89–97.